

Magnetocaloric Properties of the Ising nanotube

Ümit Akıncı¹

Department of Physics, Dokuz Eylül University, TR-35160 Izmir, Turkey

1 Abstract

The magnetocaloric properties of the Ising nanotube constituted by arbitrary core spin values S_c and the shell spin values S_s have been investigated by mean field approximation. During this investigation, several quantities have been calculated, such as isothermal magnetic entropy change, full width at half maximum value and the refrigerant capacity. The variation of these quantities with the values of the spins and exchange interaction between the core and shell is determined. Besides, recently experimentally observed double peak behavior in the variation of the isothermal magnetic entropy change with the temperature is obtained for the nanotube.

2 Introduction

Magnetocaloric effect (MCE) is defined as an occurred temperature change in the material when it is subject to the magnetic field. It was first observed in Iron [1] and theoretically explained after many years [2, 3]. MCE is simply based on the variation in different contributions to the entropy. The entropy of a magnetic material is composed of three independent parts namely, the electronic part, lattice part, and magnetic part. Under adiabatic changes, the total entropy of the material is constant. This means that, occurred a change in one part of the entropy should be balanced by other parts. Then if one increases the magnetic part of the entropy by an adiabatic process, the lattice part should decrease (by an assumption of the constant electronic part of the entropy). Decreasing lattice entropy manifests itself as a reduction in the temperature of the material. In this way, one can construct a thermodynamical cycle, in which at one step the material is at the temperature T_1 and at another step it has the temperature $T_2 > T_1$.

Refrigerant capacity (RC) is the amount of heat that can be transferred from the cold end (at temperature T_1) to the hot end (at temperature T_2) in one thermodynamical cycle. This quantity is one of the quantities which measure the suitability of the magnetic material for magnetocaloric purposes. It is in relation to another quantity namely isothermal magnetic entropy change (IMEC). In order to obtain a large adiabatic temperature change, the material should have a large IMEC, and a large RC. On the other hand a good candidate has sufficient thermal conductivity for the aim of easy heat exchange.

The typical behavior of the IMEC by the temperature includes peak at a critical temperature of the material. Generally, bulk magnetocaloric materials

¹umit.akinci@deu.edu.tr

display larger IMEC peaks but with negligible or very low RC values. On the other side, nanosystems show reduced IMEC values. But their IMEC curve spread over a wide temperature range and this fact sometimes yields larger RC (in comparison to the bulk counterparts). Thus they are promising candidates for magnetic refrigeration [4, 5]. For instance, it has been shown that the geometrical confinement of Dy and Ho can lead to an enhanced magnetocaloric effect in comparison to the bulk counterparts [6, 7]. Similarly, it has been shown for $La_{0.7}Sr_{0.3}MnO_3$ nanotube arrays, the bulk sample exhibits higher IMEC but nanotubes present an expanded temperature dependence of IMEC curves that spread over a broad temperature range [8, 9].

As explained in Sec. 3, IMEC is related to the magnetization change with the temperature. If the magnetization rapidly changes over some interval of the temperature, it is said that large MCE obtained. Nanotubes are promising materials for obtaining efficient MCE. For instance, large MCE, associated with the sharp change in magnetization of the Gd_2O_3 nanotubes has been shown experimentally [10, 11]. Another example of experimental MCE in nanotubes is the structural defect-induced MCE in $Ni_{0.3}Zn_{0.7}Fe_2O_4$ graphene (NZF/G) nanocomposites [12].

As seen in these examples, experimental studies are up to date for MCE in nanotubes. Although, MCE in nano systems is an active research area for experimentalists, to the best of our knowledge MCE on nanotube geometry has not been worked out, theoretically. But, from the theoretical side both of the magnetic behavior of these systems well studied. After the first theoretical treatments of the Ising model on nanotube geometry [13] by effective field approximation, the first results for the anisotropic Heisenberg model on nanotube geometry have been obtained within the same methodology [14]. As studied in this work in terms of the MCE, mixed spin models have been worked out for obtaining the magnetic properties. The magnetic properties of the spin (1/2-1) mixed system on nanotube geometry has been worked out within the improved mean-field approximation [15] and Monte Carlo simulation [16, 17, 18]. Also hysteresis and magnetic properties of the spin-1/2 spin-1 nanowire have been determined by Monte Carlo simulations [19]. The magnetic and hysteresis behaviors of the higher spin models are also well known theoretically.

The magnetic properties of the spin-1 and spin 3/2 nanotube has been determined within the Monte Carlo simulation [20] and quantum simulation treatment [21]. The same model on the nanowire geometry has been investigated by Monte Carlo simulation [22]. Spin (1/2-3/2) model on nanotube geometry has been investigated within the effective field theory [23] and on a nanowire geometry by Monte Carlo simulation [24, 25]. The magnetic phase transition characteristics and hysteresis behaviors of spin-3/2 spin -5/2 model on Ising nanowire have been determined by the Monte Carlo simulation [26, 27]. Besides, hysteresis and compensation behaviors of mixed spin-2 and spin-1 hexagonal Ising nanowire have been studied within the Monte Carlo simulation [28].

The aim of this work is to determine the MCE characteristics of the magnetic nanotube, by solving the Ising model with several different spin values. For this aim, the paper is organized as follows: In Sec. 3 we briefly present the model

and formulation. The results and discussions are presented in Sec. 4, and finally Sec. 5 contains our conclusions.

3 Model and Formulation

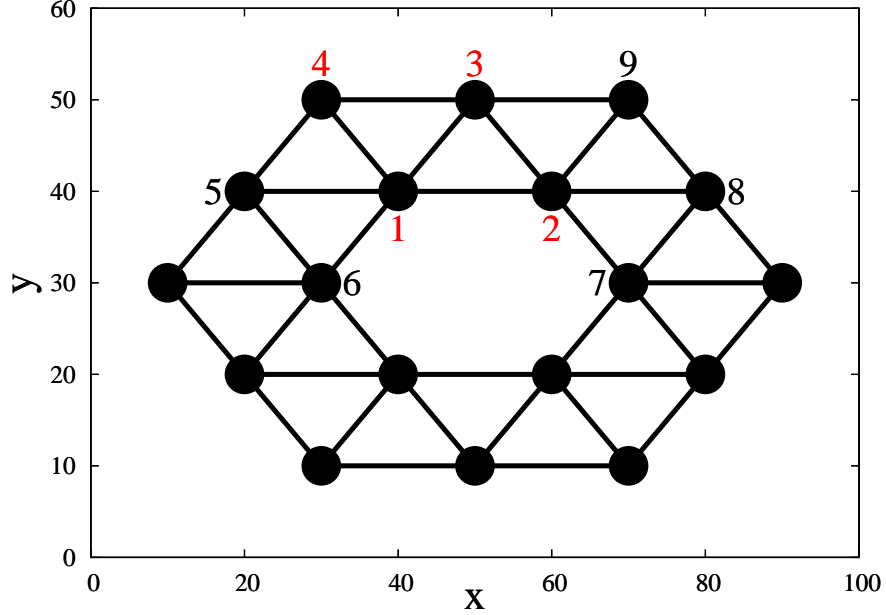


Figure 1: Schematic representation of one layer of the nanotube in xy plane. The system periodically extends in z direction.

We can see the schematic representation of the one layer of the nanotube in Fig. (1). As seen in Fig. (1), one layer of the nanotube consists of two hexagons which is called core (inner hexagon) and the shell (outer hexagon). Let the core spins have value S_c and shell spins have S_s . We can write the Hamiltonian of this system as

$$\mathcal{H} = -J_c \sum_{\langle i,j \rangle} (S_i^c S_j^c) - J_s \sum_{\langle i,j \rangle} (S_i^s S_j^s) - J_{cs} \sum_{\langle i,j \rangle} (S_i^c S_j^s) - H \sum_i S_i \quad (1)$$

where S_i^c, S_i^s denote the z component of the Pauli spin operator at a site i which belongs to the core (c) and shell (s), respectively. J_c is the exchange interaction between the nearest neighbor core spins, J_s is the exchange interaction between the nearest neighbor shell spins, and J_{cs} is the exchange interaction between the nearest neighbor core and shell spins. The former three sums in Eq. (1) are

taken over the nearest neighbor sites, while last summation is taken over all the lattice sites. In Eq. (1), H is the longitudinal magnetic field.

In order to include the effect of all exchange interactions, we take four spin cluster. We can construct one layer of the nanotube by repetition of this selected cluster. The nanotube consists of repeating layers (seen in Fig. (1)) in z direction. The Hamiltonian of this cluster (which consists of red colored spins in Fig. (1)) is

$$\mathcal{H}^{(4)} = -J_c(S_1S_2) - J_s(S_3S_4) - J_{cs}(S_1S_3 + S_1S_4 + S_2S_3) \quad (2)$$

$$-H\sum_{i=1}^4S_i - \sum_{i=1}^4h_iS_i.$$

Here, h_i are the local fields that represent the interaction of the i^{th} spin with nearest neighbor spins that belong to outside of the cluster. These local fields represent the following spin-spin interactions:

$$\begin{aligned} h_1 &= J_c(S_6 + S_{11} + S_{12}) + J_{cs}S_5 \\ h_2 &= J_c(S_7 + S_{21} + S_{22}) + J_{cs}(S_8 + S_9) \\ h_3 &= J_s(S_9 + S_{31} + S_{32}) \\ h_4 &= J_s(S_5 + S_{41} + S_{42}). \end{aligned} \quad (3)$$

Here the spins which are denoted as S_{ij} , where $i = 1, 2, 3, 4$ and $j = 1, 2$ represent the neighbor spins of the spin denoted as S_i , which are in the upper and lower plane in z direction. The thermal average of the quantity Ω can be calculated via the exact generalized Callen-Suzuki identity [29]

$$\langle \Omega \rangle = \left\langle \frac{Tr_4 \Omega \exp(-\beta \mathcal{H}^{(4)})}{Tr_4 \exp(-\beta \mathcal{H}^{(4)})} \right\rangle \quad (4)$$

In Eq. (4) Tr_4 stands for the partial trace over all the lattice sites which belong to the selected cluster and $\beta = 1/(kT)$ where k is the Boltzmann constant and T is the temperature.

Let us denote the basis set for this finite cluster by $\{|\phi_i\rangle\} = |s_1s_2s_3s_4\rangle$, where s_k is just one spin eigenvalue of the operator S_k ($k = 1, 2, 3, 4$). In this representation of the basis set, operators in the 4-spin cluster acts on the bases via

$$S_k |s_1s_2s_3s_4\rangle = s_k |s_1s_2s_3s_4\rangle, \quad (5)$$

where $k = 1, 2, 3, 4$. Note that, since the system consist of spin- S_c core and spin- S_s shell particles, number of bases equals to $(2S_c + 1)^2 (2S_s + 1)^2$.

Indeed calculation of Eq. (4) is trivial, since the matrix $\mathcal{H}^{(4)}$ is diagonal for the Hamiltonian given in Eq. (2), in the chosen basis set. The diagonal element related to the base $|s_1s_2s_3s_4\rangle$ (which can be obtained by applying operator Eq. (2) to bases according to Eq. (5)) is given by

$$\begin{aligned} \langle \phi_i | \mathcal{H}^{(4)} | \phi_i \rangle = & -J_c (s_1 s_2) - J_s (s_3 s_4) - J_{cs} (s_1 s_3 + s_1 s_4 + s_2 s_3) \\ & - H \sum_{i=1}^4 s_i - \sum_{i=1}^4 h_i s_i. \end{aligned} \quad (6)$$

Let us denote this element as $H^{(4)}(s_1, s_2, s_3, s_4)$, then we can write Eq. (4) as

$$\langle S_k \rangle = \left\langle \frac{\sum_{\{s_1, s_2, s_3, s_4\}} s_k \exp(-\beta H^{(4)}(s_1, s_2, s_3, s_4))}{\sum_{\{s_1, s_2, s_3, s_4\}} \exp(-\beta H^{(4)}(s_1, s_2, s_3, s_4))} \right\rangle, k = 1, 2, 3, 4. \quad (7)$$

The summations are taken over all the possible configurations of (s_1, s_2, s_3, s_4) . The core (m_c), shell (m_s) and total (m) magnetizations can be calculated via

$$m_c = \frac{1}{2} (\langle S_1 \rangle + \langle S_2 \rangle), \quad m_s = \frac{1}{2} (\langle S_3 \rangle + \langle S_4 \rangle), \quad m = \frac{1}{3} (m_c + 2m_s). \quad (8)$$

Up to this point, all equations are exact. But how can local fields in Eq. (6) be treated? Since our aim is to obtain some general qualitative results about the MCE in nanotube system, it is enough to treat these local fields in a level of mean field, i.e. by writing operators in Eq. (3) as their thermal averages,

$$\begin{aligned} h_1 &= J_c (2m_1 + m_2) + J_{cs} m_3 \\ h_2 &= J_c (m_1 + 2m_2) + J_{cs} (m_3 + m_4) \\ h_3 &= J_s (2m_3 + m_4) \\ h_4 &= J_s (m_3 + 2m_4). \end{aligned} \quad (9)$$

Note that, the periodicity of the lattice has been used for obtaining the expressions of local fields given in Eq. (9) from Eq. (3). In other words,

$$\begin{aligned} \langle S_{11} \rangle = \langle S_{12} \rangle = \langle S_7 \rangle &= m_1 \\ \langle S_{21} \rangle = \langle S_{22} \rangle = \langle S_6 \rangle &= m_2 \\ \langle S_{31} \rangle = \langle S_{32} \rangle = \langle S_5 \rangle = \langle S_8 \rangle &= m_3 \\ \langle S_{41} \rangle = \langle S_{42} \rangle = \langle S_9 \rangle &= m_4. \end{aligned} \quad (10)$$

By using this approximation, Eq. (7) gets the form

$$m_k = \frac{\sum_{\{s_1, s_2, s_3, s_4\}} s_k \exp(-\beta H^{(4)}(s_1, s_2, s_3, s_4))}{\sum_{\{s_1, s_2, s_3, s_4\}} \exp(-\beta H^{(4)}(s_1, s_2, s_3, s_4))}, k = 1, 2, 3, 4, \quad (11)$$

where the definitions of local fields given by Eq. (9) have been used in matrix elements $H^{(4)}(s_1, s_2, s_3, s_4)$. Then, the magnetizations m_1, m_2, m_3, m_4 can be found by numerical solution of the nonlinear equation system given by Eq. (11). Core, shell and the total magnetization can be obtained by using Eq. (8). Note that, the formulation used here is a generalization of the traditional mean-field to a larger cluster. The effect of using larger clusters can be found in Ref. [30].

In order to determine the magnetocaloric properties of the system, we calculate the isothermal magnetic entropy change (IMEC) when maximum applied longitudinal field is H_{max} , which is given by [31]

$$\Delta S_M = \int_0^{H_{max}} \left(\frac{\partial m}{\partial T} \right)_H dH. \quad (12)$$

The other quantity of interest is the refrigerant capacity which is defined by [32]

$$q = - \int_{T_1}^{T_2} \Delta S_M (T)_H dT. \quad (13)$$

Here T_1 and T_2 are chosen as those temperatures at which the magnetic entropy change gains the half of the peak value and this is called as the full width at half maximum value (FWHM) of the IMEC. This is also an important quantity of the MCE.

4 Results and Discussion

We want to focus on the magnetocaloric properties of the system. The Hamiltonian of the system includes four parameters, as one can see from Eq. (1). In order to make it possible for investigation, we have to reduce this number of parameters. For this aim let us choose $J_c = J_s = J$. By this unit of energy J (which is positive) we can work with scaled quantities as

$$r = \frac{J_{cs}}{J}, \quad h = \frac{H}{J}, \quad t = \frac{k_B T}{J}. \quad (14)$$

Note that, $h_{max} = 1.0$ is chosen in the calculations.

First, we want to elaborate on IMEC behavior for differently structured nanotubes. For this aim, we depict the variation of the IMEC with the temperature for several nanotubes constituted by core spin value $S_c = 1/2$ in Fig. (2) and $S_c = 7/2$ in Fig. (3). Each figure contains different shell spin values (S_s) and core-shell exchange interaction values (r), which are shown in the related figure. We can see from Fig. (2) that, when the spin value of the shell increases, the maximum value of the IMEC occurs in higher temperatures, and the peak value (i.e. height of the peak) of the IMEC decreases. At the same time, the curve gets wider, i.e. FWHM increases. This is consistent with the general relation between the spin value of the model and IMEC behavior. As demonstrated in

Ref. [36], when the spin value of the model increases, the height of the peak in IMEC decreases, but the curves get wider, i.e. FWHM increases.

Besides for lower values of r , the double peak behavior of the curve takes attention (see Figs. (2) (a) and (b)). This double peak behavior is depressed when the interaction of the core-shell gets stronger (see Figs. (2) (c) and (d)). Very recently, this behavior is obtained for the bilayer system experimentally [33]. Besides, double peak behavior has been obtained theoretically for bilayer [34] and superlattice systems [35].

The same double peak behavior can be seen for the system constituted by spins $S_c = 7/2$ (Fig. (3)). But the evolution of the curves by changing shell spin value is slightly different from the nanotubes that have $S_c = 1/2$, for the nanotubes that have $S_c = 7/2$ as a core spin value (see Fig. (3)). When the shell spin value increases, the peak value of IMEC increases.

For non-interacting core-shell, two peaked behavior of IMEC occurs, as seen in Figs. (2) (a) and (3) (a). For non-interacting case, the system consists of two independent layer which have spin values S_c and S_s . The low temperature peak seen in Fig.(2) (a) is related to the system with spin value of S_c and other peak is related to the system with spin value S_s . Since $S_s > S_c$ in Fig. (2) (a), it is natural for the peak related to the S_s to lie right side of the peak related to S_c in $(|\Delta S_M|, t)$ plane, due to the relations between the critical temperatures of layers that have different spin values. The same reasoning holds also for Fig.(3) (a). When the interaction between the core and shell increases, one peak behavior takes place (compare Figs.(2) (d) by (a), and Figs.(3) (d) by (a)). While this transition, the peak that occurs at lower temperature values suppressed (compare Figs.(2) (b) by (a), and Figs.(3) (b) by (a)).

To take a closer look at the IMEC behaviors with the spin value and the value of core-shell interaction, we calculate the maximum value (height of the peak) of the IMEC for different nanotubes which can be seen in Fig. (4). At first sight, height of the peak of IMEC for a certain S_c occurs at $S_s = S_c$ regardless of the value of r . Thus, as seen in Fig. (4) decreasing trend with rising S_s occurs for $S_c = 1/2$ and increasing trend with rising S_s occurs for $S_c = 7/2$. For the values of $1/2 < S_c < 7/2$, rising S_s rises the height of the peak of IMEC until $S_s = S_c$, after then rising S_s causes to a decline in the height of the peak of IMEC. We can see similar behavior for FWHM in Fig. (5). Except $(S_c, S_s) = (5/2, 1/2), (3, 1/2), (7/2, 1/2)$ nanotubes, rising S_s first decreases FWHM, minimum FWHM occurs at $S_s = S_c$, after then rising S_s causes to increment behavior in FWHM.

For refrigerant capacity defined in Eq. (13), we depict the same scatter plot in Fig. (6). As we can see from Fig. (6), rising S_s cause increasing refrigerant capacity for spin values of core provide $S_c < 3$. If the core spin value exceeds $5/2$, slightly lowering behavior takes place for larger shell spin values. Interestingly, weak interaction between the core and the shell causes larger refrigerant capacity for higher spin values (compare gray dots by black dots in $S_c = 3$ and $7/2$).

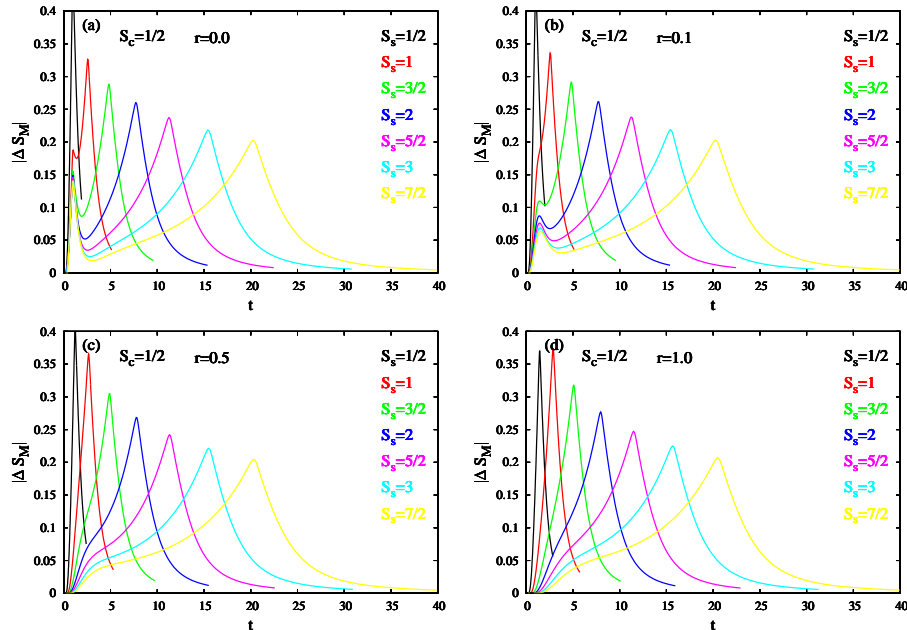


Figure 2: The variation of IMEC with the temperature for selected values of $S_s = 1/2, 1, 3/2, 2, 5/2, 3, 7/2$ and $r = 0.0, 0.1, 0.5, 1.0$ for nanotube that have core spin value of $S_c = 1/2$.

5 Conclusion

The MCE properties of the Ising nanotube constituted by arbitrary core spin values S_c and the shell spin values S_s have been investigated by mean field approximation. During this investigation, several quantities have been calculated, such as IMEC, FWHM and the refrigerant capacity (q). The variation of these quantities with the values of the spins and exchange interaction between the core and shell is determined.

First general conclusions about the variation of the IMEC with the temperature has been obtained. As consistently by the conclusions obtained in Ref. [36] for the general spin valued Ising model on a regular lattice, it is observed that when the spin values of the nanotube increase, the height of the peak in IMEC decreases. This peak occurs at the critical temperature of the system, as expected. Besides, for a chosen spin value for the core, increasing shell spin value yields rising height of the peak in IMEC, when $S_c = S_s$ maximum value is obtained. After that (i.e. $S_c < S_s$), increasing spin value of the shell yields decreasing behavior in the height of the peak in IMEC. Completely reverse evolution occurs in FWHM, when the value of the shell spin increases. On the other hand, refrigerant capacity has increasing trend in the conditions of rising

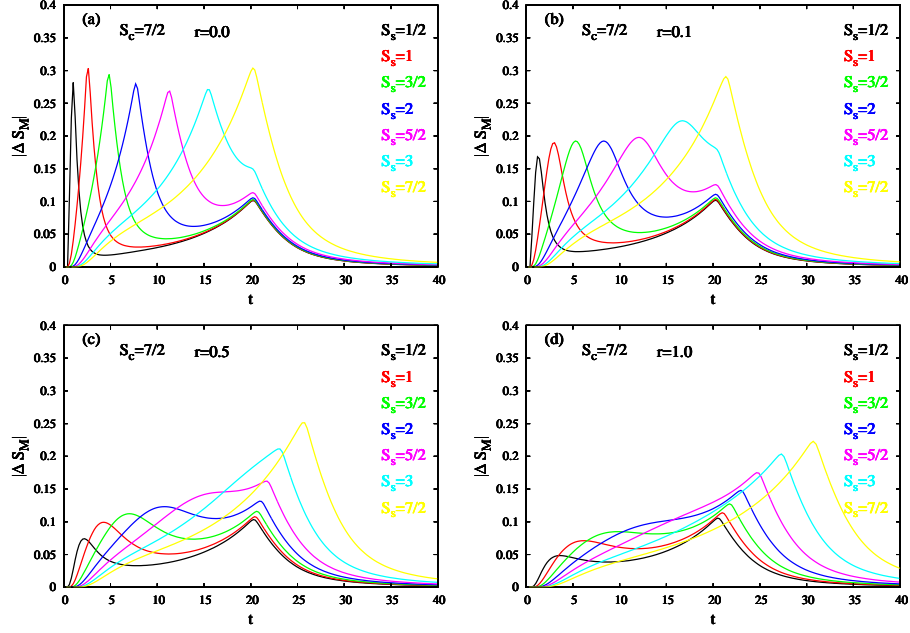


Figure 3: The variation of IMEC with the temperature for selected values of $S_s = 1/2, 1, 3/2, 2, 5/2, 3, 7/2$ and $r = 0.0, 0.1, 0.5, 1.0$ for nanotube that have core spin value of $S_c = 7/2$.

core and shell spin values. These observations may yield a tuning of MCE in nanotube system. Although it is very hard task to tune the interaction between the core and shell experimentally, theoretical knowledge about the relation between the spin values (or exchange interaction between the core and the shell) and MCE characteristics may yield important experimental achievements.

Other than these results, recently obtained double peak behavior in IMEC for bilayer system is observed in nanotube system also. The physical explanation is briefly discussed.

We hope that the results obtained in this work may be beneficial form both theoretical and experimental point of view.

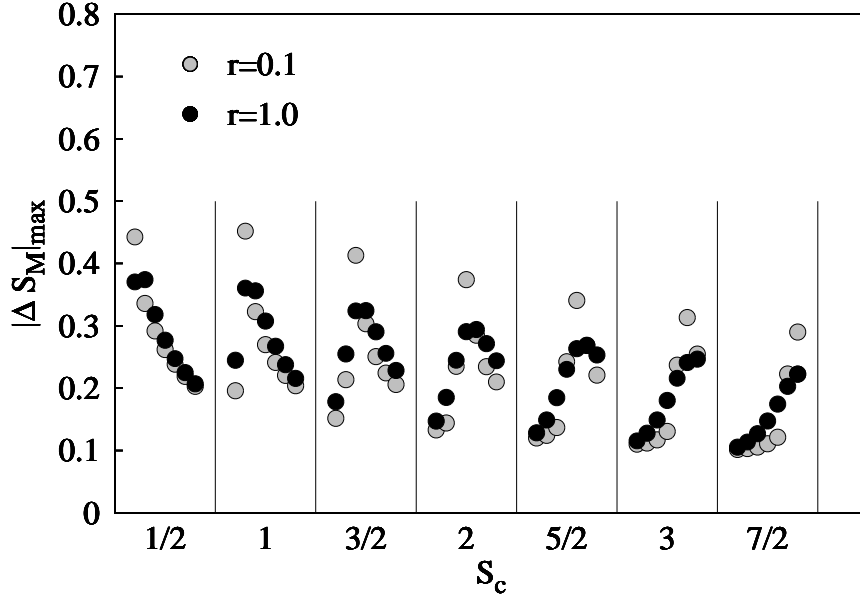


Figure 4: The maximum value of the IMEC for nanotubes that consist of spin values $S_c, S_s = 1/2, 1, 3/2, 2, 5/2, 3, 7/2$ and for selected values of $r = 0.1, 1.0$. Each box labeled by S_c contains number of 7 circles for certain value of r . Each circle corresponds to different values of S_s , starting from $S_s = 1/2$ (most left), by increment value of $1/2$ and arrive $S_s = 7/2$ (most right) in a box.

References

- [1] E. Warburg, Ann. Phys. 13, 141 (1881).
- [2] P. Debye, Ann. Phys. 81, 1154 (1926).
- [3] W. F. Giauque, J. Amer. Chem. Soc. 49, 1864 (1927).
- [4] Akhter, S. et al. J. Magn. Magn. Mater. 2014, 367, 75-80.
- [5] Chaudhary, V. et al J. Appl. Phys. 2014, 116, 163918.
- [6] V. Mello, A. L. Dantas, and A. Carrico, Solid State Commun. 140, 447 (2006).
- [7] F. C. M. Filho, V. D. Mello, A. L. Dantas, F. H. S. Sales, and A. S. Carrico, J. Appl. Phys. 109, 07A914 (2011)
- [8] M. Kumaresavanji et al, APPLIED PHYSICS LETTERS 105, 083110 (2014)

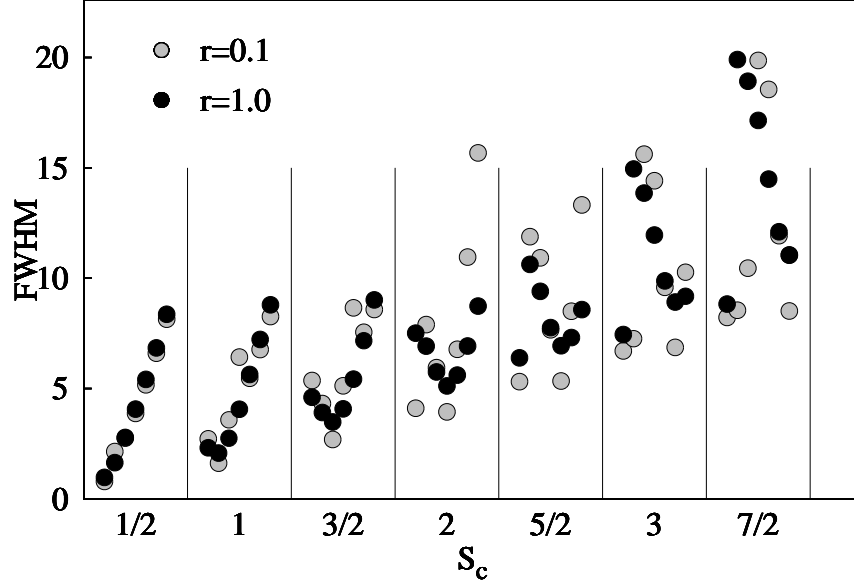


Figure 5: The value of FWHM for nanotubes that consist of spin values $S_c, S_s = 1/2, 1, 3/2, 2, 5/2, 3, 7/2$ and for selected values of $r = 0.1, 1.0$. Each box labeled by S_c contains number of 7 circles for certain value of r . Each circle corresponds to different values of S_s , starting from $S_s = 1/2$ (most left), by increment value of $1/2$ and arrive $S_s = 7/2$ (most right) in a box.

- [9] M. Kumaresavanji et al JOURNAL OF APPLIED PHYSICS 117, 104304 (2015)
- [10] Rima Paul et al, Journal of Magnetism and Magnetic Materials 417 (2016) 182-188
- [11] Rima Paul et al, Physica E 80 (2016) 149-154
- [12] T. Prabhakaran et al. J. Phys. Chem. C 2019, 123, 25844-25855
- [13] T. Kaneyoshi Phys. Status Solidi B 248, No. 1, 250-258 (2011)
- [14] U. Akinci arXiv:1308.2511 [cond-mat.stat-mech] (2014)
- [15] R.G.B. Mendes, F.C. Sá Barreto, J.P. Santos Physica A 505 (2018) 1186-1195
- [16] R.G.B. Mendes, F.C. Sá Barreto, J.P. Santos Journal of Magnetism and Magnetic Materials 471 (2019) 365-369

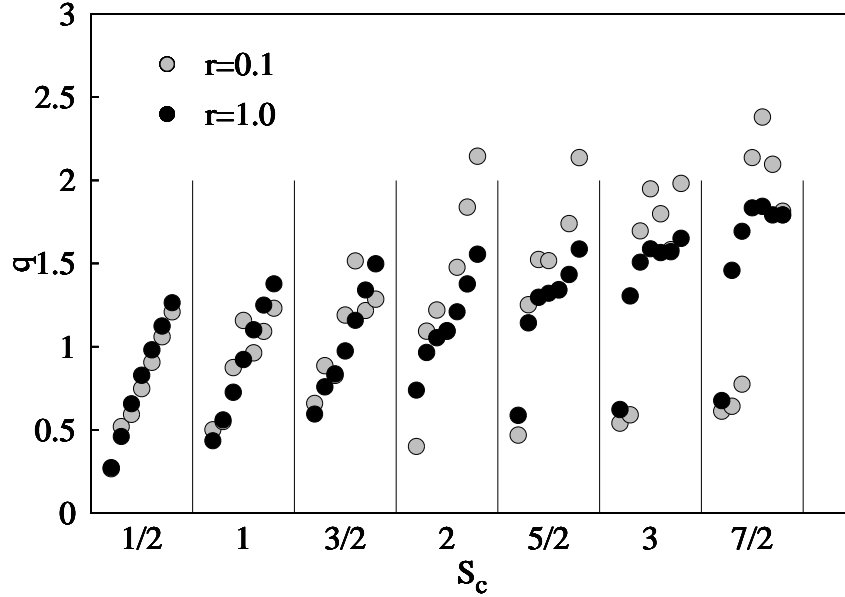


Figure 6: The value of the refrigerant capacity (q) for nanotubes that consist of spin values $S_c, S_s = 1/2, 1, 3/2, 2, 5/2, 3, 7/2$ and for selected values of $r = 0.1, 1.0$. Each box labeled by S_c contains number of 7 circles for certain value of r . Each circle corresponds to different values of S_s , starting from $S_s = 1/2$ (most left), by increment value of $1/2$ and arrive $S_s = 7/2$ (most right) in a box.

- [17] M. Boughrara , M. Kerouad, A. Zaim Journal of Magnetism and Magnetic Materials 360 (2014) 222-228
- [18] M. Boughrara , M. Kerouad, A. Zaim Physica A 433 (2015) 59-65
- [19] A. Oubelkacem et al. Physica B 549 (2018) 82-86
- [20] R. Masrour and A. Jabar EPL, 128 (2019) 46002
- [21] Zhaosen Liu , Hou Ian Physica E 85 (2017) 82-89
- [22] Feraoun, A. Kerouad, M. Appl. Phys. A 124, 735 (2018).
- [23] Ferhat Taşkın et al., Physica A 407 (2014) 287-294
- [24] B. Boughazi, M. Boughrara , M. Kerouad Physica A 465 (2017) 628-635
- [25] Hachem, N et al, J Supercond Nov Magn 31, 2165-2172 (2018)
- [26] J D Alzate-Cardona et al 2017 J. Phys.: Condens. Matter 29 445801

- [27] Rachid Aharrouch et al, Multidiscipline Modeling in Materials and Structures in Press DOI: 10.1108/MMMS-11-2019-0194
- [28] R. Masrour et al Physica B 472 (2015) 19-24
- [29] T. Balcerzak, J. Magn. Magn. Mater. 246 (2002) 213.
- [30] Ü Akıncı, Journal of Magnetism and Magnetic Materials, 386, 60-68 (2015)
- [31] A.M. Tishin, Y.I. Spichkin, The Magnetocaloric Effect and Its Applications, Institute of Physics, 2003.
- [32] K.A. Gschneidner Jr., V.K. Pecharsky, Annu. Rev. Mater. Sci. 30 (2000) 387.
- [33] Ruihao Yuan et al J. Appl. Phys. 127, 154102 (2020)
- [34] Karol Szalowski, Tadeusz Balcerzak Thin Solid Films 534, (2013), 546-552
- [35] Ping Xu, An Du Physica B 521 (2017) 134-140
- [36] Ü. Akıncı, Y. Yüksel, E. Vatansever, Physics Letters A, 382 3238-3243 (2018)